

# Scaling of Selfavoiding Tethered Membranes: 2-Loop Renormalization Group Results

François David<sup>†</sup> and Kay Jörg Wiese

Service de Physique Théorique, C.E.A. - Saclay, 91191 Gif-sur-Yvette Cedex, France  
(February 6, 2008)

The scaling properties of selfavoiding polymerized membranes are studied using renormalization group methods. The scaling exponent  $\nu$  is calculated for the first time at two loop order.  $\nu$  is found to agree with the Gaussian variational estimate for large space dimension  $d$  and to be close to the Flory estimate for  $d = 3$ .

The statistical properties of polymerized flexible membranes are interesting and still poorly understood [1]. These objects arise either in a collapsed (fractal dimension  $d_f = 3$ ), a crumpled swollen ( $2 < d_f < 3$ ) or a flat ( $d_f = 2$ ) phase. The physical properties of such membranes in three dimensions can be studied by experiments and computer-simulations. Most of the simulations find a flat phase [2–6], due to an induced effective curvature term (stiffness) of the membrane [3]. A swollen phase with fractal dimension near to the Flory-prediction  $d_f = 2.5$  has been found by exactly balancing curvature terms with a long-range repulsive interaction, thus interpreting the swollen phase as a tricritical point [5]. The experimental results are contradictory. In [7] but not in [8] a swollen phase is found.

An analytical approach inspired from polymer theory [11], which relies on renormalization group and  $\varepsilon$ -expansion methods, was initiated in [9,10], where it was used to perform calculations at 1-loop order. Its consistency to all orders in perturbation theory has been established in [12]. In this letter we present the first application of this method to 2-loop calculations and discuss the results obtained by this approach.

The membrane is modeled by a continuum model à la Edwards: the embedding of the  $D$ -dimensional membrane in  $d$ -dimensional bulk space is described by the mapping  $x \in R^D \rightarrow \vec{r}(x) \in R^d$ . The renormalized Hamiltonian is

$$\mathcal{H}[\vec{r}] = \frac{Z}{2} \int_x (\nabla \vec{r}(x))^2 + b Z_b \mu^\varepsilon \int_x \int_y \delta^d(\vec{r}(x) - \vec{r}(y)) , \quad (1)$$

where  $b$  is the dimensionless renormalized coupling constant,  $\mu$  the renormalization momentum scale and  $\varepsilon = 2D - d(2 - D)/2$ . Physical quantities are calculated perturbatively in  $b$ . Direct calculations for  $D = 2$  for membranes are not possible, since perturbation theory

is singular;  $D$  and  $d$  have therefore to be treated as continuous variables and an  $\varepsilon$ -expansion must be performed. The renormalization factors  $Z(b, \varepsilon)$  and  $Z_b(b, \varepsilon)$  are introduced in order to subtract the short-distance divergences which appear as poles in  $\varepsilon$  at the critical dimension  $\varepsilon = 0$ .

At order  $b^n$  one has to calculate the expectation value with respect to the free theory ( $b = 0$ ) of  $n$  bilocal operators, henceforth called dipoles:  $x \longleftrightarrow y = \delta^d(\vec{r}(x) - \vec{r}(y))$  integrated over the whole membrane. Short-distance divergences occur when dipole end-points approach each other. The most important tool to deal with these divergences is the multilocal operator product expansion (MOPE) [12], which describes all possible contractions of dipoles to the operators marginal at  $\varepsilon = 0$ . Power counting shows that there are only two such operators: the dipole operator and the local operator:  $\frac{1}{2}(\nabla r(x))^2 = \dagger_x$ . For instance, the contraction of a dipole to a point generates  $\dagger$  with the MOPE coefficient

$$\left( \left( \begin{array}{c} \text{dipole} \\ \text{---} \\ \text{---} \\ \text{---} \end{array} \right) \middle| \dagger \right) = -\frac{1}{2D} |x - y|^{\varepsilon - D} . \quad (2)$$

The integral over the relative distance of the two points is UV-divergent. As in [18] we use the minimal subtraction scheme to subtract these divergences. Introducing an IR-cutoff  $L \propto \mu^{-1}$  the Feynman-diagram becomes

$$\left\langle \left( \begin{array}{c} \text{dipole} \\ \text{---} \\ \text{---} \\ \text{---} \end{array} \right) \middle| \dagger \right\rangle_L = \int_{\substack{\text{all distances} \\ \text{smaller than } L}} \left( \begin{array}{c} \text{dipole} \\ \text{---} \\ \text{---} \\ \text{---} \end{array} \right) \middle| \dagger \right) . \quad (3)$$

Our strategy is to keep  $D$  fixed and to expand (3) as a Laurent series in  $\varepsilon$ , which here starts at  $\varepsilon^{-1}$ . Denoting by  $\langle \mid \rangle_{\varepsilon^p}$  the term of order  $\varepsilon^p$  of  $\langle \mid \rangle_{L=1}$ , the counterterms are chosen to have pure poles in  $\varepsilon$ , and for instance the first counterterm corresponding to (2) is

$$\left\langle \left( \begin{array}{c} \text{dipole} \\ \text{---} \\ \text{---} \\ \text{---} \end{array} \right) \middle| \dagger \right\rangle_{\varepsilon^{-1}} = -\frac{1}{2D} \frac{1}{\varepsilon} .$$

Extending this analysis along the lines of [12] leads to the following results (details will be given elsewhere [19]). To second order, the counterterms which render the theory finite are found to be

$$Z = 1 - \left\langle \left( \begin{array}{c} \text{dipole} \\ \text{---} \\ \text{---} \\ \text{---} \end{array} \right) \middle| \dagger \right\rangle_{\varepsilon^{-1}} b + \left[ \left\langle \left( \begin{array}{c} \text{dipole} \\ \text{---} \\ \text{---} \\ \text{---} \end{array} \right) \middle| \dagger \right\rangle_{\varepsilon^{-2}, \varepsilon^{-1}} - 2 \left\langle \left( \begin{array}{c} \text{dipole} \\ \text{---} \\ \text{---} \\ \text{---} \end{array} \right) \middle| \dagger \right\rangle_{\varepsilon^{-1}} \left\langle \left( \begin{array}{c} \text{dipole} \\ \text{---} \\ \text{---} \\ \text{---} \end{array} \right) \middle| \dagger \right\rangle_{\varepsilon^{-1}, \varepsilon^0} \right]$$


$$+ \left\langle \left( \text{diagram 1} \right) \middle| \left( \text{diagram 2} \right) \right\rangle_{\varepsilon^{-1}}^2 \left\langle \left( \text{diagram 3} \right) \middle| \left( \text{diagram 4} \right) \right\rangle_{\varepsilon^0} - 2 \left\langle \left( \text{diagram 5} \right) \middle| \left( \text{diagram 6} \right) \right\rangle_{\varepsilon^{-1}} \left\langle \left( \text{diagram 7} \right) \middle| \left( \text{diagram 8} \right) \right\rangle_{\varepsilon^0} \right] \frac{b^2}{2!} \quad (4)$$

$$Z_b = 1 + 2 \left\langle \left( \text{diagram 9} \right) \middle| \left( \text{diagram 10} \right) \right\rangle_{\varepsilon^{-1}} \frac{b}{2!} - \left[ 4 \left\langle \left( \text{diagram 11} \right) \middle| \left( \text{diagram 12} \right) \right\rangle_{\varepsilon^{-2}, \varepsilon^{-1}} - 12 \left\langle \left( \text{diagram 13} \right) \middle| \left( \text{diagram 14} \right) \right\rangle_{\varepsilon^{-1}} \left\langle \left( \text{diagram 15} \right) \middle| \left( \text{diagram 16} \right) \right\rangle_{\varepsilon^{-1}, \varepsilon^0} + 12 \left\langle \left( \text{diagram 17} \right) \middle| \left( \text{diagram 18} \right) \right\rangle_{\varepsilon^{-2}, \varepsilon^{-1}} - 12 \left\langle \left( \text{diagram 19} \right) \middle| \left( \text{diagram 20} \right) \right\rangle_{\varepsilon^{-1}} \left\langle \left( \text{diagram 21} \right) \middle| \left( \text{diagram 22} \right) \right\rangle_{\varepsilon^{-1}, \varepsilon^0} \right] \frac{b^2}{3!} \quad (5)$$

Following [12], the renormalization group  $\beta$ -function and the anomalous scaling dimension  $\nu$  of  $\vec{r}$  are obtained from the variation of the coupling constant and the field with respect to the renormalization scale  $\mu$ , keeping the bare couplings fixed. They are written in terms of  $Z$  and  $Z_b$  as

$$\beta(b) = \frac{-\varepsilon b}{1 + b \frac{\partial}{\partial b} \ln Z_b + \frac{d}{2} b \frac{\partial}{\partial b} \ln Z} \quad (6)$$

$$\nu(b) = \frac{2-D}{2} - \frac{1}{2} \beta(b) \frac{\partial}{\partial b} \ln Z \quad (7)$$

In order to compute these coefficients, we apply our methods of [18], which must be extended in order to deal with the double poles in  $\varepsilon^{-2}$  from subdivergences. We demonstrate the method using the example of the counterterm associated with the diagram  $\mathcal{G} =$  



$$\left\langle \left( \text{diagram G} \right) \middle| \left( \text{diagram H} \right) \right\rangle_L = L^{2\varepsilon} \left[ \frac{c_2}{\varepsilon^2} + \frac{c_1}{\varepsilon} + \mathcal{O}(\varepsilon^0) \right] \quad (8)$$

A subdivergence occurs when the single dipole to the right of the diagram  $\mathcal{G}$  is contracted to a point. According to the MOPE of [12], when this contraction is performed *first*, the MOPE coefficient factorizes as

$$\left( \text{diagram G} \right) \approx \left( \text{diagram I} \right) \times \left( \text{diagram J} \right) \quad (9)$$

This implies that the double pole of (8) is the same as the double pole appearing in the product of the counterterms associated with the two diagrams on the r.h.s. of (9)

$$L^{2\varepsilon} \left[ \frac{c_2}{\varepsilon^2} + \frac{\tilde{c}_1}{\varepsilon} + \mathcal{O}(\varepsilon^0) \right] = \frac{1}{2} \left\langle \left( \text{diagram I} \right) \middle| \left( \text{diagram H} \right) \right\rangle_L \left\langle \left( \text{diagram J} \right) \middle| \left( \text{diagram H} \right) \right\rangle_L \quad (10)$$

The factor 1/2 comes from the nested integration [13], arising from the fact that the double pole is given by the r.h.s. of (9), integrated with the restriction  $\mathcal{R}$  that the distance in  is smaller than all the distances in . As a consequence, we can extract the difference of the residues of the single poles,  $c_1 - \tilde{c}_1$ , by subtracting to the l.h.s. of (8) a counterterm proportional to the r.h.s. of (9), *restricted to the domain*  $\mathcal{R}$ . In fact, this combination has to be calculated, see (5). We get:

$$L^{2\varepsilon} \left[ \frac{c_1 - \tilde{c}_1}{\varepsilon} + \mathcal{O}(\varepsilon^0) \right] = \int_{\substack{\text{distances} \\ \leq L}} \left( \text{diagram G} \right) - \int_{\substack{\{\text{distances}\} \cap \mathcal{R} \\ \leq L}} \left( \text{diagram I} \right) \times \left( \text{diagram J} \right) \quad (11)$$

The careful reader will have remarked that (10) and the last term in (11) are calculated with a slightly different regularization prescription. The difference however is of order  $\varepsilon^0$  and thus does not change the result [19].  $c_1 - \tilde{c}_1$  is now extracted by applying  $L \frac{\partial}{\partial L}$  to the r.h.s. of (11) and taking the limit  $\varepsilon \rightarrow 0$ . We then obtain

$$c_1 - \tilde{c}_1 = \frac{L}{2} \lim_{\varepsilon \rightarrow 0} \left[ \int_{\substack{\text{largest} \\ \text{distance} = L}} \left( \text{diagram G} \right) - \int_{\substack{\text{largest} \\ \text{distance} = L}} \left( \text{diagram I} \right) \times \left( \text{diagram J} \right) \right] \quad (12)$$

This integral is locally finite and can be reduced to an integral over five independent distances between pairs of points. We evaluate it by applying and extending the numerical techniques of [18]. The main difficulty thereby comes from the fact that although convergent, the integral (12) has integrable singularities, which have to be removed by suitable variable transformations and mappings between domains of integration. Finally the in-

tegrand has large variations in some small subdomains and can only be integrated by a genuine adaptive Monte Carlo integration. For analytical and numerical details we refer the reader to [18,19].

The other diagrams appearing in (4) and (5) are calculated similarly. Having performed all numerical calculations ( $\sim 10^3$ h CPU on a WorkStation), the renormalization-group functions  $\beta(b)$  and  $\nu(b)$  can be

calculated.  $\beta(b)$  has a non-trivial IR-fixed point for  $b = b_c > 0$  (i.e.  $\beta(b_c) = 0$  and  $\beta'(b_c) > 0$ ). The full dimension of the field  $\nu$  at this critical point,  $\nu(b_c)$  is a function of  $D$  and  $\varepsilon$ :

$$\nu(D, \varepsilon) = \frac{2-D}{2} + \nu_1(D)\varepsilon + \nu_2(D)\varepsilon^2 + \mathcal{O}(\varepsilon^3) \quad (13)$$

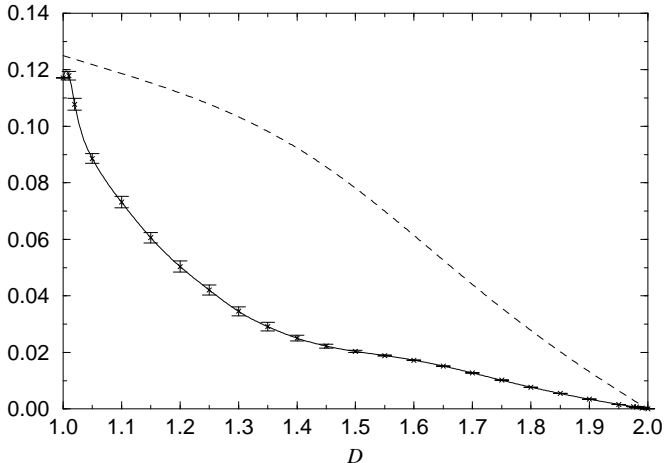


FIG. 1. The functions  $\nu_1(D)$  (dashed line) and  $\nu_2(D)$  (solid line). The latter is given with the statistical error.

The coefficients are plotted in figure 1. Naively setting  $D = 2$  and  $d = 3$ , i.e.  $\varepsilon = 4$  in equation (13), yields the wrong result 0. To obtain the correct result, one has to redevelop this expansion around any point  $(D_0, d_0 = \frac{4D_0}{2-D_0})$  on the critical curve ( $\varepsilon = 0$ ). We use a generalization of the methods introduced in [20]. Note that the expansion (13) is exact in  $D$  and of order 2 in  $\varepsilon$ , thus can be expanded up to order 2 in  $D - D_0$  and  $\varepsilon$ . Given any invertible transformation  $\{x, y\} = \{x(D, \varepsilon), y(D, \varepsilon)\}$ , one can express  $D$  and  $\varepsilon$  as function of  $x$  and  $y$  and re-expand up to order 2 in  $x$  and  $y$ . The goal is to find a set of variables, such that the estimate for  $\nu$  depends the least on the choice of the expansion point on the critical curve and which reproduces well the known results in the following cases:  $D = 1$ ,  $D = d$  and  $d \rightarrow \infty$  (see below). The sets  $\{D, D_c(d) = \frac{2d}{4+d}\}$  and  $\{D_c(d), \varepsilon\}$  have been found to be good choices. The plot in figure 2 shows the value of  $\nu$  as a function of the expansion point  $\{D, d_c(D) = 4D/(2-D)\}$  on the critical curve. The prediction at 1-loop order (dashed line) is essentially independent of the expansion point. At 2-loop order the estimate starts from the 1-loop result at  $D = 2$ , grows until it reaches a plateau around  $D = 1.5$  and then grows rapidly again. This is a general feature of this kind of expansion and can well be studied by applying the same method to the Flory-estimate  $\nu_{\text{Flory}} = (2 + D)/(2 + d)$ . In this case the plateau becomes flatter if one goes to higher orders but does not cover the whole range, i.e. the expansion is not convergent for all  $D$ . To extract  $\nu$  from figure 2, one uses the maximum and the minimum of the

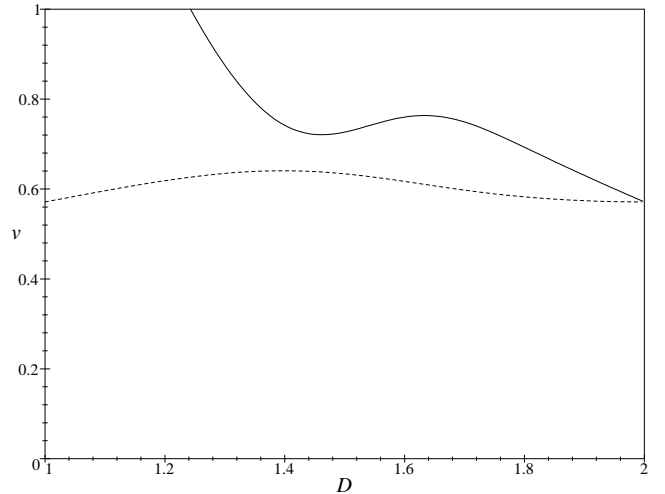


FIG. 2. Extrapolation of  $\nu$  via (13) in  $D_c(d)$  and  $\varepsilon$  for membranes  $D = 2$  in  $d = 3$ . The first order results are given by the dashed line, the second order by the solid line.

plateau. Their mean is an estimate for  $\nu$ , their difference an estimate of the error in *this* expansion scheme. We get  $\nu = 0.74 \pm 0.02$ . It must be emphasized that different sets of variables yield different values for  $\nu$ .

One possibility to further improve the extrapolation is to develop  $\nu d$  or  $\nu(d + 2)$ . The first is interesting, as it calculates corrections around the estimate predicted by a Gaussian variational ansatz [21],  $\nu_{\text{var}} = 2D/d$ :

$$\nu(b_c)d = 2D + \left( \beta(b) \frac{\partial}{\partial b} \ln Z_b(b) \right) \Big|_{b=b_c} \quad (14)$$

The smaller  $\ln(Z_b)$  is, the more accurate the expansion becomes. At 1- and 2-loop order  $\ln(Z_b)$  vanishes like  $\exp(-\text{const}/d)$  for large  $d$ . We argue that this persists to any order in perturbation theory. For large  $d$ ,  $\nu_{\text{var}}$  thus becomes exact.

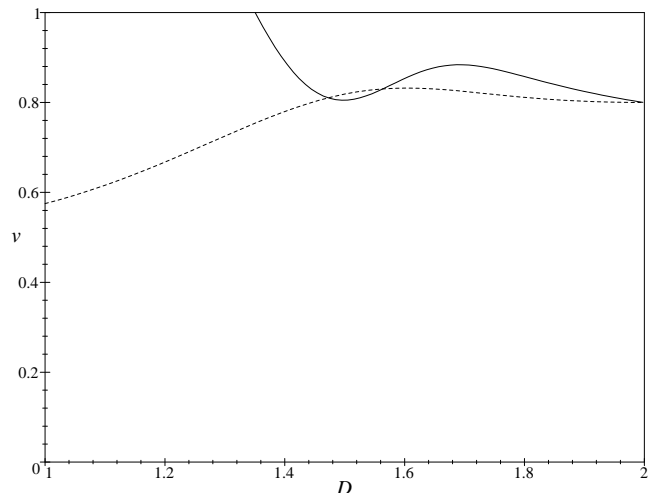


FIG. 3. Extrapolation of  $\nu$  via (15) in  $d$  and  $\varepsilon$  for membranes  $D = 2$  in  $d = 3$ . The first order results are given by the dashed line, the second order by the solid line.

The second possibility is a systematic expansion around the Flory-estimate  $\nu_{\text{Flory}} = (D + 2)/(d + 2)$ :

$$\nu(b_c)(d + 2) = D + 2 + \left( \beta(b) \frac{\partial}{\partial b} \ln \left( \frac{Z_b}{Z} \right) \right) \Bigg|_{b=b_c} \quad (15)$$

The Flory-estimate is excellent for polymers and one hopes [20] that it is also good for membranes. Therefore the corrections should be small. Such an extrapolation is given in figure 3. The estimate for  $\nu$  is slightly larger than that in figure 2.

The results of a 2-loop extrapolation for  $\nu$  are presented in figure 4 for membranes ( $D = 2$ ) in  $d$ -dimensions ( $2 \leq d \leq 20$ ).

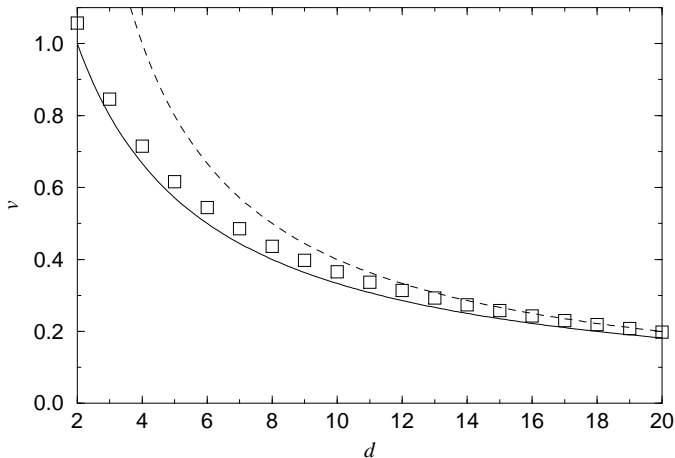


FIG. 4. Extrapolation of the 2-loop results in  $d$  and  $\varepsilon$  for membranes  $D = 2$  in  $d$  dimensions, using (15) (squares). The solid line is the prediction made by Flory's theory, the dashed line by the variational ansatz.

We see that for  $d \rightarrow \infty$  the prediction of the Gaussian variational method becomes exact, as argued above. For small  $d$ , the prediction made by Flory's argument is close to our results. This is a non-trivial result, since the membrane case corresponds to  $\varepsilon = 4$  and in comparison with polymers in  $d = 3$ , where  $\varepsilon = 1/2$ , the 2-loop corrections were expected to be large. In fact we have found that they are small when one expands around the critical curve  $\varepsilon = 0$  for an adequate range of  $D \sim 1.5$  (depending slightly on  $d$  and on the choice of variables) and a suitable choice of extrapolation variables. In this case the 2-loop corrections are even smaller than the 1-loop corrections and allow for more reliable extrapolations to  $\varepsilon = 4$ .

In conclusion, we have presented here the first renormalization group calculation at 2-loop order for self-avoiding flexible tethered membranes. In order to improve these results, one should understand if the plateau phenomenon observed at 2-loop order persists to higher orders, and one should control the general large order behavior of perturbation theory for this model. Another important issue is whether the IR-fixed point studied here

is stable towards perturbation by bending rigidity. Indeed, it has been argued [3] that for small enough  $d$  this might destabilize the crumpled phase and explain why numerical simulations in  $d = 3$  normally see a flat phase.

## ACKNOWLEDGMENTS

We thank E. Gutter and J. Zinn-Justin for useful discussions and E. Gutter and Chitra for a careful reading of the manuscript.

<sup>†</sup> Member of CNRS

- [1] *Statistical Mechanics of Membranes and Surfaces*, Proceedings of the Fifth Jerusalem Winter School for Theoretical Physics (1987), D. R. Nelson, T. Piran and S. Weinberg Eds., World Scientific, Singapore (1989).
- [2] F. F. Abraham, W. E. Rudge and M. Plischke, *Phys. Rev. Lett.* **62** (1989) 1757.
- [3] F. F. Abraham and D. R. Nelson, *J. de Physique* **51** (1990) 2653; *Science* **249** (1990) 393.
- [4] G. S. Grest and M. Murat, *J. de Physique* **51** (1990) 1415.
- [5] G. S. Grest and I. B. Petsche, *Phys. Rev.* **E 50** (1994) R1737-1740
- [6] D.M. Kroll and G. Gompper, *J. Phys. I France* **3** (1993) 1131
- [7] T. Hwa, E. Kokufuta, T. Tanaka, *Phys. Rev.* **A 44**, (1994) R2235-2238, X. Wen et al., *Nature* 355 (1192) 426
- [8] M. S. Spector, E. Naranjo, S. Chiruvolu and J. A. Zasadzinski *Phys. Rev. Lett.* **73** 21 (1994) 2867
- [9] J. A. Aronowitz and T. C. Lubensky, *Europhys. Lett.* **4** (1987) 395.
- [10] M. Kardar and D. R. Nelson, *Phys. Rev. Lett.* **58** (1987) 1289; *Phys. Rev.* **A 38** (1988) 966.
- [11] J. des Cloizeaux and G. Jannink, *Polymers in solution, their modelling and structure*, Clarendon Press, Oxford, (1990).
- [12] F. David, B. Duplantier and E. Gutter, *Phys. Rev. Lett.* **72** (1994) 311.
- [13] This point is already explained (without using the MOPE formalism) in B. Duplantier, T. Hwa and M. Kardar, *Phys. Rev. Lett.* **64** (1990) 2022.
- [14] F. David, B. Duplantier and E. Gutter, in preparation.
- [15] B. Duplantier, *Phys. Rev. Lett.* **62** (1989) 2337.
- [16] F. David, B. Duplantier and E. Gutter, *Nucl. Phys.* **B 394** (1993) 555
- [17] F. David, B. Duplantier and E. Gutter, *Phys. Rev. Lett.* **70** (1993) 2205.
- [18] K.J. Wiese and F. David, *Nucl. Phys.* **B 450** (1995) 495
- [19] F. David and K. J. Wiese, in preparation.
- [20] T. Hwa, *Phys. Rev.* **A41** (1990) 1751
- [21] E. Gutter and J. Palmeri, *Phys. Rev.* **A 45**, (1992) 734